

# Extinction and Near-Extinction Instability of Non-Premixed Tubular Flames

Shengteng Hu<sup>1</sup>, Robert W. Pitz<sup>2</sup> and Yu Wang<sup>3</sup>

*Mechanical Engineering Department, Vanderbilt University, Nashville, TN 37235 USA*

**Tubular non-premixed flames are formed by a novel opposed tubular burner, which has proven to be a valuable tool to study the effects of curvature on flames. Extinction of the opposed tubular flames generated by burning inert-gases-diluted H<sub>2</sub>, CH<sub>4</sub> or C<sub>3</sub>H<sub>8</sub> with air is investigated for both concave and convex curved cases. Data are made available in terms of the critical fuel dilution ratios at various stretch rates. N<sub>2</sub>, He, Ar or CO<sub>2</sub> diluent is used. The onset conditions of the cellular instability are recorded. The effects of curvature on both flame extinction and cellularity are discussed.**

## I. Introduction

Flame extinction is important for both turbulent combustion and fire safety.<sup>1</sup> Four types of extinction, namely extinction by stretch rate, extinction by dilution, extinction by convective heat transfer, and extinction by radiation,<sup>2</sup> are of interest to researchers with the first two attracting the most attention. Extinction of the counterflow diffusion flame in the forward stagnation region of a porous cylinder immersed in a uniform air stream was one of the earliest studies.<sup>3-6</sup> Extinction measurements of non-premixed flames utilizing opposed-jet burners were more commonly utilized by researchers.<sup>7-9</sup> Typically, the limiting fuel and oxidizer concentrations using various diluents varying with injection velocities (or strain rates) were measured as the extinction limits. Numerical investigation of the extinction of diffusion flames with detailed chemistry started in the 1980's. Extinction prediction on the Tsuji type burner using complex chemistry and detailed formulation of the transport fluxes were performed as a collaborated efforts by five research groups<sup>10</sup> and the results compared well with the measured values.<sup>5,11</sup> Similar numerical efforts on the opposed-jet burner can be found elsewhere.<sup>12-14</sup>

While research on extinction of the non-premixed flames subject to the effects of flame stretch and non-unity Lewis number abounds, experimental studies on the effects of curvature are less numerous. This is mainly because of the difficulties in establishing a simple geometry that will allow detailed investigations. Despite the difficulties, efforts, including studies on the tip-opening of Burke-Schumann flames<sup>15-19</sup> and perturbed opposed-jet flames<sup>20-23</sup>, have been made to investigate the curvature effects on flame extinction. It was discovered that curvature has only minor effects on the tip-opening of the Burke-Schumann flame, where the effects of preferential diffusion dominants. Curvature plays a more important role in the flame/vortex interaction, but studies were qualitative in nature due to 1) the non-uniform curvature along the flame surface; 2) the transient nature of the problem under investigation in some cases.

Despite the rich discoveries in the previous experimental and numerical studies, the effects of curvature on extinction deserve more attention. By installing a nozzle along the center axis of the tubular burner as a second, radially-outwardly flowing reactant source, non-premixed and partially-premixed flames subject to well-controlled aerodynamic straining and flame curvature can be created.<sup>24</sup> This burner possesses the advantages over the above-mentioned methods in that it allows a more detailed quantitative study of the non-premixed flame subject to the influences of both uniform stretch and uniform curvature. It offers the capability of investigating the effects of curvature on the flame extinction, which constitutes the first objective of this study. Numerical simulation is also carried out and compared with the experimental data.

Flames at near extinction conditions often exhibit instability, which leads to cellular structure and/or oscillation. Cellular instability of non-premixed flames has been reported by several researchers using various types of burners. One of the earliest studies was reported by Dongworth and Melvin,<sup>25</sup> where a Wolfhard-Parker burner was used. Flames produced by hydrogen/nitrogen-air exhibited cellular structure at a certain fuel dilution ratio. The authors

---

<sup>1</sup> Graduate Student, Mechanical Engineering Department, Student Member.

<sup>2</sup> Chair and Professor, Mechanical Engineering Department, Associate Fellow.

<sup>3</sup> Graduate Student, Mechanical Engineering Department, Student Member.

postulated that inter-lancing of the non-premixed stream and the premixed stream of fuel and oxidizer through inter-stream diffusion at the flame base produced a non-uniform distribution of fuel at the flame base, and was therefore responsible for the occurrence of cellularity, although the factors determining the size of the cells was not clearly identified. Ishizuka and Tsuji observed a striped pattern for hydrogen-nitrogen/air flames established in the Tsuji-type burner, where the flame resided in the fuel side of the stagnation point.<sup>4</sup> The authors attributed this phenomenon to the preferential diffusion of  $H_2$  relative to  $N_2$  in the fuel mixture and claimed that it closely resembled a similar discovery in premixed flames. Cellular instability and flame extinction using a slot-jet burner were systematically studied by Chen et al., where hydrogen, methane and propane diluted with a variety of inert diluents were used.<sup>26</sup> Based on the experimental results, they proposed that near-extinction and sufficiently low Lewis number of the deficient reactant stream ( $Le \leq 0.8$ ) were the two requirements for flame to exhibit cellular instability. The Lewis number (diffusive-thermal) effect in a manner similar to that of premixed flames was argued to be the driving force instead of the effects of preferential diffusion. The diffusive-thermal instability of non-premixed flames was further investigated in a counterflow slot jet burner at low Lewis number.<sup>27</sup> A tube-like flame generated by the balance between flame weakening due to strain and intensification due to curvature was reported for the  $H_2/N_2$ -air flames. Flame tubes of various states were observed under various flow configurations. In a more recent study,<sup>28</sup> cell formation in non-premixed, axisymmetric jet flames near extinction was investigated in detail, where much attention was drawn upon the influence of initial mixture strength  $\phi$  to the selection criteria of cellular patterns. A theoretical study on the diffusional-thermal instability of diffusion flames using activation-energy asymptotics was first started by Kim, Williams and Ronney,<sup>29</sup> and additional contributions can be found from several researchers.<sup>30-32</sup>



**Figure 1. Axial integrated image of the concave  $H_2-N_2$ /air opposed tubular flame at  $X_F=18.8\%$ ,  $K=53 \text{ s}^{-1}$ ,  $R_s \approx 6.5 \text{ mm}$  (upper part of the image is blocked by the inner nozzle).**

Cellular structure in opposed tubular flames has been reported in previous studies<sup>24</sup> for flames produced by non-unity Lewis number reactants. It was shown that the flame instability originated from the effects of curvature and Lewis number. However, a systematic investigation on the near-extinction behavior of non-premixed tubular flames was not conducted. The second objective of this study is to characterize the cellularity of the opposed tubular flames burning  $N_2$ , He, Ar or  $CO_2$  diluted  $H_2$ ,  $CH_4$  or  $C_3H_8$  against air. The initial mixture strength (calculated as the fuel-to-oxygen molar ratio normalized by the stoichiometric molar ratio) and stretch rate at the stagnation surface are used as parameters to describe the cellular instability.

## II. Experimental Method

An opposed tubular burner with outer nozzle diameter of 30 mm and inner nozzle diameter of 6.4 mm is employed, where the heights of both nozzles are 20 mm (Fig. 2). A detailed description of the burner can be found elsewhere.<sup>24,33</sup> Fuel mixtures are formed by diluting  $H_2$ ,  $CH_4$  or  $C_3H_8$  with  $N_2$ , He, Ar or  $CO_2$ . The fuel-diluent combinations attempted in this study are summarized in Table 1. The fuel + diluent mixture is sent through the inner nozzle flowing outward, and oxidizer, which is always air, is sent through the outer nozzle flowing inward. The only exception is a  $H_2 + N_2$  case, where the fuel and oxidizer flows are switched in order to generate flames with opposite curvature as shown in Table 1.

A mirror with a slot-cut is mounted underneath the tubular burner at 45 degrees to the axis of symmetry, which provides a view of the flame in the axial direction. An infrared sensitive ICCD video camera (Xyberion ISG-250) mounted horizontally toward the mirror records the axially-integrated chemiluminescence emission from the flames to monitor the extinction and cellular structure. A typical picture of the flame recorded is shown in Fig. 1,

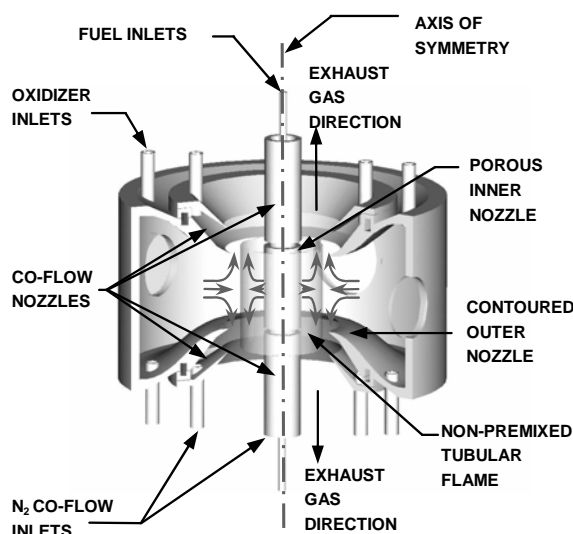


**Figure 2. Schematic of the opposed tubular burner**

where the upper part of the circle is missing due to the presence of the inner nozzle. The gas flows are controlled by mass flow controllers (Teledyne Hastings HFC-202/203) through a computer. During the experiment, a non-premixed tubular flame is ignited at a fuel concentration that is slightly higher than its corresponding extinction value, and then the fuel concentration is decreased in steps of 0.1-0.2% of the full scale of the flow controllers until extinction is reached. There are only a few cases where the flame is started at a lower diluent level and then the flow rate of the diluent is gradually increased until extinction is reached. All gas flows are supplied at room temperature 297 K.

**Table 1. Summary of experimental conditions and relevant parameters.**

Fuel	Diluent	$R_s^1$ , mm	$X_F^2$ , %	$K^3$ , $s^{-1}$	$\phi^4$	$Le_F^5$	$a^6$	CV <sup>7</sup>	CL <sup>8</sup>
CH <sub>4</sub>	N <sub>2</sub>	5.0	14.9 - 26.3	24.4 - 218	1.42 - 2.51	1.02 - 1.03	0.64 - 0.34	CA	N
		6.5	15.3 - 49.5*	16.7 - 172	1.46 - 4.71	1.02 - 1.05	0.62 - 0.16	CA	N
		8.0	15.6 - 21.0	18.2 - 89.2	1.49 - 2.00	1.02	0.61 - 0.44	CA	N
CH <sub>4</sub>	He	5.0	15.8 - 37.2	107 - 270	1.50 - 3.55	1.72 - 1.09	0.14 - 0.08	CA	N
		6.5	20.8 - 34.0	47.1 - 193	1.98 - 3.24	1.54 - 1.16	0.11 - 0.09	CA	N
CH <sub>4</sub>	Ar	5.0	10.1 - 18.6	35.2 - 163	0.96 - 1.78	0.96	1.35 - 0.69	CA	N
		6.5	10.2 - 19.5	24.6 - 150	0.97 - 1.86	0.96	1.34 - 0.66	CA	N
CH <sub>4</sub>	CO <sub>2</sub>	5.0	25.1 - 32.0	21.4 - 113	2.39 - 3.04	0.82 - 0.86	0.54 - 0.40	CA	N
		6.5	24.2 - 33.7	22.4 - 88.0	2.30 - 3.21	0.81 - 0.87	0.56 - 0.37	CA	N
		8.0	24.0 - 38.3	28.1 - 129	2.29 - 3.65	0.81 - 0.90	0.57 - 0.32	CA	N
C <sub>3</sub> H <sub>8</sub>	N <sub>2</sub>	5.0	6.16 - 14.3	22.9 - 180	1.47 - 3.40	1.76 - 1.51	0.69 - 0.31	CA	N
		6.5	6.90 - 15.7	25.0 - 196	1.64 - 3.74	1.74 - 1.47	0.62 - 0.29	CA	N
		8.0	7.33 - 17.9*	20.0 - 142	1.75 - 4.27	1.72 - 1.41	0.58 - 0.25	CA	N
H <sub>2</sub>	N <sub>2</sub>	5.0	10.7 - 16.9*	25.2 - 172	0.25 - 0.40	0.37 - 0.42	3.46 - 2.03	CA	Y
		6.5	9.08 - 16.9*	19.4 - 214	0.22 - 0.40	0.35 - 0.42	4.12 - 2.03	CA	Y
		8.0	8.56 - 10.3	30.4 - 90.9	0.20 - 0.25	0.35 - 0.37	4.38 - 3.57	CA	Y
H <sub>2</sub>	N <sub>2</sub>	5.0	6.43 - 7.99	35.6 - 96.0	0.15 - 0.19	0.33 - 0.34	5.97 - 4.73	CX	Y
		6.5	7.35 - 8.61	26.4 - 106	0.18 - 0.21	0.34 - 0.35	5.17 - 4.36	CX	Y
		8.0	11.2 - 12.5	56.6 - 227	0.27 - 0.30	1.10	0.49 - 0.44	CA	N
H <sub>2</sub>	He	5.0	10.3 - 13.1	154 - 465	0.25 - 0.31	1.10 - 1.09	0.54 - 0.42	CA	N
		6.5	10.5 - 13.1	71.0 - 380	0.25 - 0.31	1.10 - 1.09	0.52 - 0.42	CA	N
		8.0	11.2 - 12.5	56.6 - 227	0.27 - 0.30	1.10	0.49 - 0.44	CA	N
H <sub>2</sub>	Ar	5.0	8.93 - 10.6	34.6 - 205	0.21 - 0.25	0.35 - 0.37	5.95 - 4.92	CA	Y
		6.5	7.29 - 9.19	23.9 - 216	0.17 - 0.22	0.33 - 0.35	7.41 - 5.77	CA	Y
H <sub>2</sub>	CO <sub>2</sub>	5.0	14.6 - 15.8	41.8 - 138	0.35 - 0.38	0.29	3.79 - 3.44	CA	Y
		6.5	12.1 - 20.6*	25.9 - 131	0.29 - 0.49	0.26 - 0.34	4.67 - 2.50	CA	Y

1 Radius of the stagnation surface based on the cold flow condition

2 Mole concentration of fuel at nozzle outlet

3 Stretch rate at the fuel side of the stagnation surface

4 Mole-based initial mixture strength, fuel-to-oxygen molar ratio normalized by the stoichiometric molar ratio

5 Lewis number of the fuel stream

6 Mass-based initial mixture strength, oxygen-to-fuel mass ratio normalized by the stoichiometric mass ratio

7 Direction of curvature, CA: concave; CX: convex

8 Cellularity, Y: yes; N: no

\* Effects of heat losses at low stretch rates.

The radius of curvature at the stagnation surface of the cold flow,  $R_s$ , given by Wang et al.,<sup>34</sup> is a function of the inlet radii, density, and velocity of the two opposing streams. As a result, the radius of curvature of the flame can be controlled by varying the velocity ratio of the two nozzles at given nozzle radii and the flow density ratio. In this study, three  $R_s$  representing different degree of curvature effects are realized for different fuel/diluent mixtures as summarized in Table 1.

The influence of the flow rate of N<sub>2</sub> co-flow is evaluated and can be neglected. The mass flow controllers have an 1% full scale accuracy. For each extinction and instability onset data point presented hereafter, the experiments are repeated at least three times and the mean values are used. The uncertainties are estimated based on the standard deviation of the measured data and the accuracy of the mass flow controllers, i.e. the maximum of the above two values are used and shown as error bars on the subsequent figures. The uncertainties are generally less than 3%, although in some cases, bigger uncertainties can be observed.

### III. Experimental Results and Discussion

Extinction data for different fuel-diluent combinations subject to various degrees of curvature are first presented and discussion is focused on extinction by stretch rate, which is represented by the upper branches of the extinction curves shown hereafter. This is followed by the experimental results for the onset of cellular structures. The stagnation stretch rate on the fuel side of the cold flow field is used as the characteristic stretch rate, and its expression can be found in Wang et al.<sup>34</sup> In the subsequent discussions, the term, concave or convex curvature always refers to the fuel stream.

#### A. Extinction

Fig. 3 shows the extinction stretch rate versus the initial mixture strength for N<sub>2</sub> diluted CH<sub>4</sub> and C<sub>3</sub>H<sub>8</sub> concave opposed tubular flames subject to various degrees of curvature. The upper branches of the curves show the effects of stretch rate on the flame, i.e. the fuel concentration needed to sustain the flame is higher as the flame is stretched more, while the lower branches show the extinction behavior due to heat losses to the inner nozzle as the reactant inlet velocities have dropped very low and flames become very thick. The upper branches have similar slopes within each fuel group. The extinction curves of both the CH<sub>4</sub>-N<sub>2</sub> and C<sub>3</sub>H<sub>8</sub>-N<sub>2</sub> mixtures subject to different degrees of curvature lie close to each other respectively, although the Lewis number for the CH<sub>4</sub>-N<sub>2</sub> is less than that of the C<sub>3</sub>H<sub>8</sub>-N<sub>2</sub> mixture (Table 1). The mass based initial mixture strength  $\alpha$ , which is calculated as oxygen-to-fuel mass ratio normalized by the stoichiometric mass ratio<sup>35</sup>, for both mixtures are less than 1 and fall within similar range. This suggests that the non-premixed flame is oxidizer deficient and flame resides on the oxidizer side of the stagnation surface. The effects of curvature are such that the flames are more resistant to extinction as they are curved more (smaller radii of curvature) as shown in Fig. 3. This has two implications: 1) the concave curvature strengthens the non-premixed flame, which leads to higher extinction stretch rates; 2) the critical Lewis number where the opposite curvature effects occur,  $Le_{cr}$ , is less than 1.

Fig. 4 shows the extinction stretch rate as function of the initial mixture strength for He, Ar or CO<sub>2</sub> diluted CH<sub>4</sub> flames subject to various degrees of curvature. Although the Lewis number goes from above one to less than one (Table 1), the extinction stretch rates for smaller R<sub>s</sub> are always higher than that for bigger R<sub>s</sub> at a given initial mixture strength, i.e. extinction curves with smaller R<sub>s</sub> are always to the left of the ones with higher R<sub>s</sub> values. Similar phenomena can also be observed in Fig. 3. This again confirms that the concave curvature strengthens these non-premixed flames. The  $\alpha$  value of both the CH<sub>4</sub>-He and CH<sub>4</sub>-CO<sub>2</sub> mixtures are less than unity, which means the flame is on the oxidizer side of the stagnation surface. Although the  $\alpha$  value of the CH<sub>4</sub>-Ar mixture goes from above one to below it, the Lewis numbers in both streams of this flame are close to unity. As a result the extinction curves lie close to each other.

It can be seen in Fig. 4 that the gap between the helium-diluted extinction curves subject to different radii

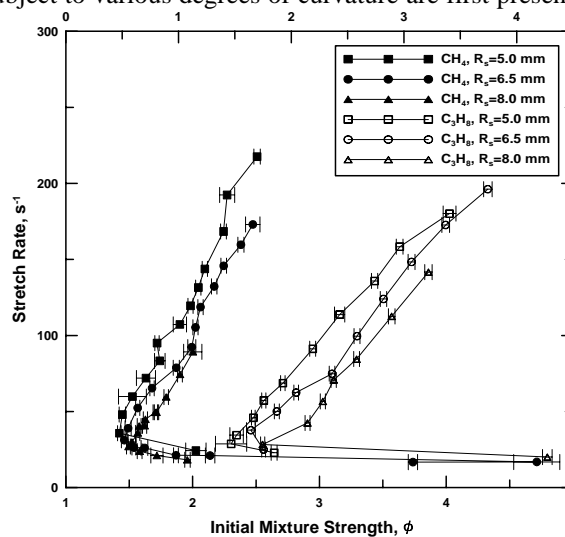


**Figure 3.** The extinction stretch rate of the opposed tubular flame as function of the initial mixture strength for various radii of the stagnation surface. Fuel: CH<sub>4</sub>/C<sub>3</sub>H<sub>8</sub>; diluent: N<sub>2</sub>; oxidizer: air. Note: CH<sub>4</sub> uses lower X-axis, C<sub>3</sub>H<sub>8</sub> uses upper one.

the concave curvature strengthens the non-premixed flame, which leads to higher extinction stretch rates; 2) the critical Lewis number where the opposite curvature effects occur,  $Le_{cr}$ , is less than 1.

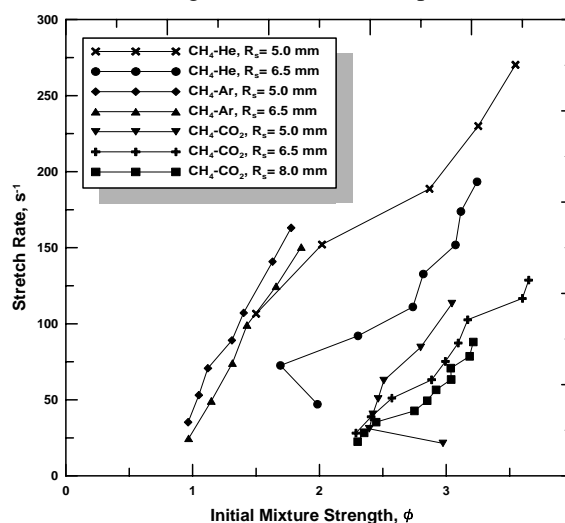


**Figure 4.** The extinction stretch rate of the opposed tubular flame as function of the initial mixture strength for two different radii of the stagnation surface and two different diluents. Fuel: CH<sub>4</sub>; diluent: He/Ar/CO<sub>2</sub>; oxidizer: air.

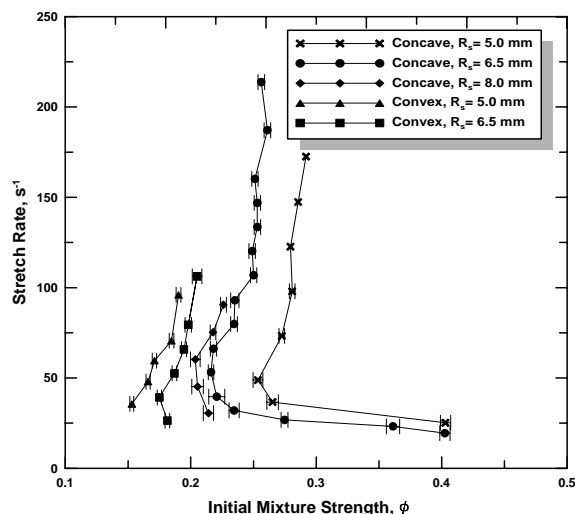


**Figure 5.** The extinction stretch rate of the opposed tubular flame as function of the initial mixture strength for various radii of the stagnation surface and different directions of curvature. Fuel: H<sub>2</sub>; diluent: N<sub>2</sub>; oxidizer: air.

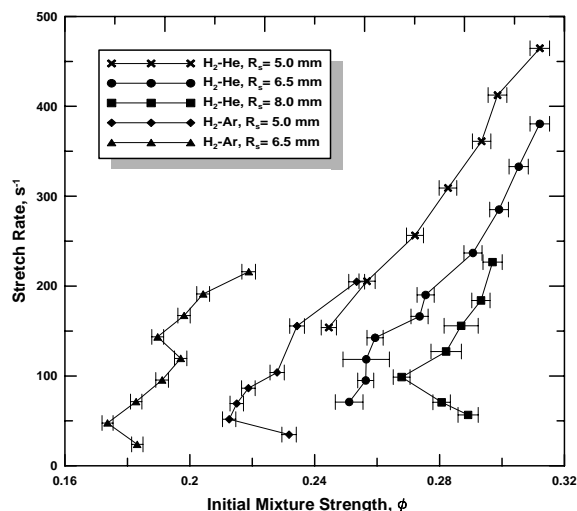


**Figure 6.** The extinction stretch rate of the opposed concave tubular flame as function of the initial mixture strength for various radii of the stagnation surface and two different diluents. Fuel: H<sub>2</sub>; diluent: He/Ar; oxidizer: air.

of curvature is wider than that of the argon or carbon dioxide diluted ones. In addition, Fig. 3 shows that at Lewis numbers close to that of the CH<sub>4</sub>-He mixture, the extinction curves of the C<sub>3</sub>H<sub>8</sub>-N<sub>2</sub> mixture lies close to each other. One possible explanation is based on the mass-based initial mixture strength  $\alpha$  and the effects of curvature. Its value for CH<sub>4</sub>-He mixture is very small comparing to the others, which indicates that this flame is extremely oxidizer deficient. This means the opposed tubular flame would reside deep in the oxidizer stream and difference between the flame radii are magnified. This will lead to the widened gap between the two curves shown in Fig. 4. Greater difficulties are encountered when trying to ignite this flame due to the increased flame instabilities, which could also contribute to this observation. Indeed, the measured results show greater variations as the initial mixture strength is increased.

The measured extinction stretch rates versus the initial mixture strength for N<sub>2</sub> diluted H<sub>2</sub> opposed tubular flames for both concave and convex curved cases are shown in Fig. 5. Concave H<sub>2</sub>-N<sub>2</sub>/air flames with smaller radii are prone to extinction, i.e. flames extinguish at higher fuel concentrations; convex H<sub>2</sub>-N<sub>2</sub>/air flames with smaller radii are more resistant to extinction, i.e. flames can exist under lower fuel concentrations. It is also shown in Fig. 5 that the convex opposed tubular flames are more resistant to extinction than the concave ones. The  $\alpha$  value of the H<sub>2</sub>-N<sub>2</sub> mixture is greater than unity, so the flame resides on the fuel side. Based on the above observations, given that the Lewis number of the H<sub>2</sub>-N<sub>2</sub> mixture falls in the range of 0.33 - 0.42 (Table 1), which is much less than unity, two conclusions can be drawn: 1) concave (convex) curvature retards (promotes) combustion, and therefore leads to early (late) extinction; 2)  $Le_{cr}$  is greater than 0.4.

For hydrogen flames using helium as diluent, the fuel Lewis number is greater than unity and the flame resides in the oxidizer stream. Based on the argument above, flames with smaller radii of curvature will be more resistant to extinction. This is confirmed by the data shown in Fig. 6, where the flames are always concave. Also shown in Fig. 6 is the extinction data for H<sub>2</sub>-Ar/air flames. The H<sub>2</sub>-Ar mixture has a fuel Lewis number much less than one, so again, the flames with bigger radii of curvature demonstrate higher extinction stretch rate at a given initial mixture strength.

## B. Cellular Instability

Cellular structures in the opposed tubular non-premixed flames have been reported previously.<sup>24</sup> However, no effort was made to quantify the onset conditions of the cellularity in the previous study. Following the same experimental procedure, these onset conditions are carefully recorded in this study. Extinction behavior is different for flames that demonstrate cellular instability. In most cases, local extinction at one angular location starts to develop and a stripped pattern is formed when the onset condition for cellularity is reached. As the initial mixture strength is decreased further, local extinction occurs at more than one angular location and flames with cell numbers

vary from 1 to 4 are observed as shown in Fig. 7. In Fig. 6 (a) - (d), the top part of the flame viewed in the axial direction is partially blocked by the inner nozzle, so not all cellular structures are readily seen. The stripped patterns that shown in Fig. (e) and (f) are taken with the CCD video camera looking in the radial direction. The strips are steady at the given experimental conditions.

Only the onset conditions of cellularity are recorded, while no data was made available to relate the cell numbers to the flow conditions as great uncertainty has been experienced in the attempt to do so. The flame with only one cell is not stable and the flame cell is always rotating. Both clockwise and counter-clockwise rotations are observed, which indicates the direction of rotation is random. Flames with 1, 3 and 4 cells show the preferred curvature property discovered previously<sup>24</sup>, but not the flames with 2 cells.

Shown in Fig. 8 are the onset boundaries of cellular structures and the regions where cellularity exists in the H<sub>2</sub>-N<sub>2</sub>/air opposed tubular flames with both concave and convex curvature. For ease of discussion, the initial mixture strength is plotted as functions of the stretch rate. Consistent with previous findings<sup>26,28</sup>, cellularity is only observed in flames close to extinction and with sufficiently low fuel stream Lewis numbers. At stretch rates not lying in the regions of extinction due to heat loss, regions of cellularity are becoming narrower as the stretch rates are raised higher. The cellularity region becomes wider as the radius of curvature is increased for the concave cases, which indicates that the concave curvature is preventing cellular structure from forming. As discussed earlier, the concave curvature retards combustion process, and the flame exhibits lower flame temperature. Flames with smaller radii of curvature extinguish earlier if the initial mixture strength is decreased gradually, so the region that

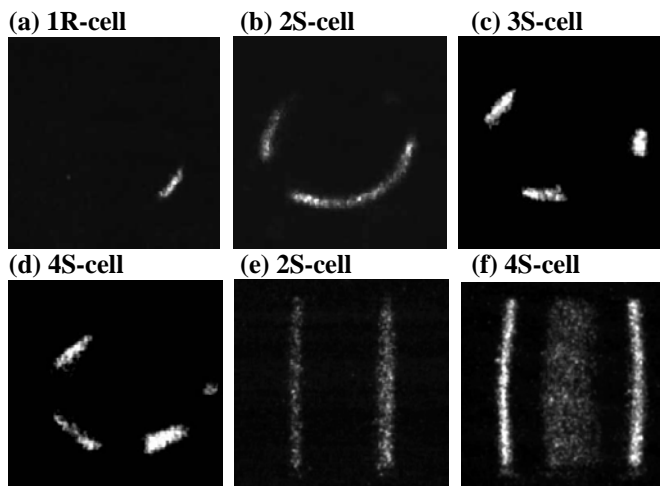


**Figure 7. Images of the cellular structure of the diluted-H<sub>2</sub>/air opposed tubular concave flame. (a) - (d): H<sub>2</sub>-N<sub>2</sub> viewed in the axial direction; (e) and (f): H<sub>2</sub>-CO<sub>2</sub> viewed in the radial direction. (a) X<sub>F</sub>≈11.4%, K≈73 s<sup>-1</sup>, R<sub>s</sub>≈5.0 mm; (b) X<sub>F</sub>=11.8%, K≈30 s<sup>-1</sup>, R<sub>s</sub>≈8.0 mm; (c) X<sub>F</sub>≈9.1%, K≈45 s<sup>-1</sup>, R<sub>s</sub>≈8.0 mm; (d) X<sub>F</sub>≈9.9%, K≈45 s<sup>-1</sup>, R<sub>s</sub>≈8.0 mm; (e) X<sub>F</sub>≈17.2%, K≈64 s<sup>-1</sup>, R<sub>s</sub>≈5.0 mm; (f) X<sub>F</sub>≈9.7%, K≈42 s<sup>-1</sup>, R<sub>s</sub>≈6.5 mm. “R” represents rotating cells and “S” stationary ones.**

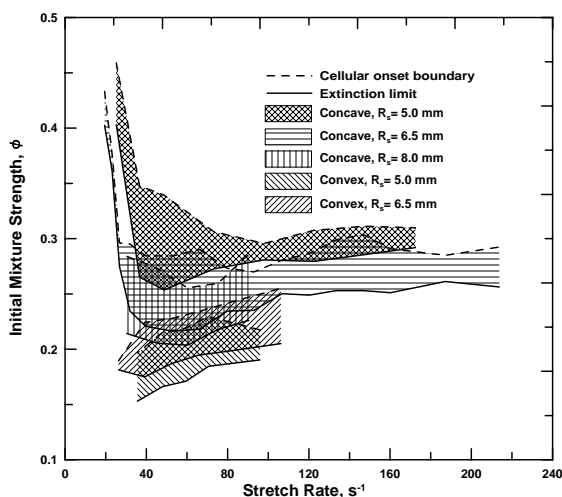


**Figure 8. The onset initial mixture strength of cellular structures and the regions where cellularity exists for opposed tubular flames plotted as functions of stretch rate with both concave and convex curvature. Fuel: H<sub>2</sub>; diluent: N<sub>2</sub>; oxidizer: air.**

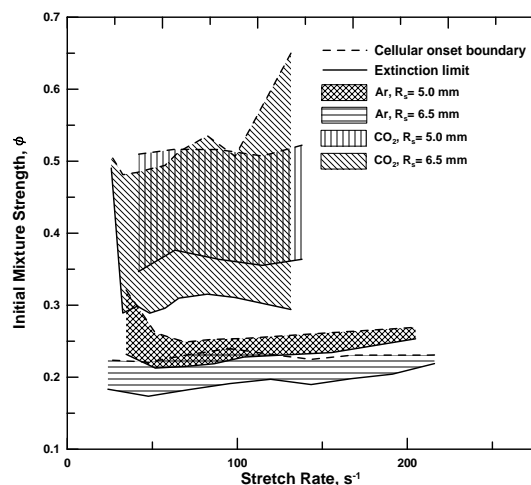


**Figure 9. The onset initial mixture strength of cellular structures and the regions where cellularity exists for opposed concave tubular flames plotted as functions of stretch rate subject to different effects of curvature. Fuel: H<sub>2</sub>; diluent: Ar/CO<sub>2</sub>; oxidizer: air.**

favors cellularity becomes smaller. The H<sub>2</sub>-Ar/air and H<sub>2</sub>-CO<sub>2</sub>/air flame data shown in Fig. 9 confirm this postulate by showing similar trends. This can also be verified by studying flames with opposite curvature. However, there are not enough data available for the convex cases due to experimental difficulties. More efforts are needed in the future.

#### IV. Conclusion

A novel opposed tubular burner is used to study the curvature effects on extinction and cellularity of non-premixed flames. The extinction limits of opposed tubular flames burning various fuel (H<sub>2</sub>, CH<sub>4</sub> or C<sub>3</sub>H<sub>8</sub>)/inert gases (N<sub>2</sub>, He, Ar or CO<sub>2</sub>) mixture with air are measured in terms of the initial mixture strength versus the stretch rate. The effects of curvature are studied by varying the radii of the flame curvature. From the data, it is discovered that the curvature effects are always coupled with the effects of the Lewis number. There exists a critical Lewis number  $Le_{cr}$ , which is less than unity such that when  $Le < (>) Le_{cr}$ , the concave curvature retards (promotes) combustion and weakens (strengthens) the non-premixed flame; vice versa for the convex curvature. The value of  $Le_{cr}$  is between 0.4 and 1. Experiments with more varieties of fuel/diluent combinations are needed to be done to determine its value.

Cellular structures with 1 to 4 cells are observed in this study for flames with sufficiently-low fuel Lewis number. Quantitative onset conditions for cellularity in non-premixed tubular flames are measured. Regions of the observed cellular instability are mapped out in the initial mixture strength - stretch rate diagram. The effects of the concave curvature are to suppress the cellular instability as shown by comparing the maps of flames with different radii of curvature.

#### Acknowledgments

The authors acknowledge funding support from NASA (NASA Grant No: NNC04AA14A) with John Brooker as the technical monitor.

#### References

- <sup>1</sup>Williams, F. A., "A Review of Flame Extinction," *Fire Safety Journal*, Vol. 3, 1981, 163-175.
- <sup>2</sup>Williams, F. A., "Progress in Knowledge of Flamelet Structure and Extinction," *Progress in Energy and Combustion Science*, Vol. 26, 2000, 657-682.
- <sup>3</sup>Tsuji, H. and Yamaoka, I., "The Counterflow Diffusion Flame in the Forward Stagnation Region of a Porous Cylinder," *Proceedings of the Combustion Institute*, Vol. 11, Berkeley, 1966, 979-984.
- <sup>4</sup>Ishizuka, S. and Tsuji, H., "An Experimental Study of Effect of Inert Gases on Extinction of Laminar Diffusion Flames," *Proceedings of the Combustion Institute*, Vol. 18, 1981, 695-703.
- <sup>5</sup>Tsuji, H., "Counterflow Diffusion Flames," *Progress in Energy and Combustion Science*, Vol. 8, 1982, 93-119.
- <sup>6</sup>Riechelmann, D., Fujimori, T. and Sato, J., "Effect of Dilution on Extinction of Methane Diffusion Flame in High Temperature Air Up to 1500 K," *Combustion Science and Technology*, Vol. 174, 2002, 23-46.
- <sup>7</sup>Puri, I. K. and Seshadri, K., "Extinction of Diffusion Flames Burning Diluted Methane and Diluted Propane in Diluted Air," *Combustion and Flame*, Vol. 65, 1986, 137-150.
- <sup>8</sup>Chen, C. L. and Sohrab, S. H., "Simultaneous Effects of Fuel/Oxidizer Concentrations on the Extinction of Counterflow Diffusion Flames," *Combustion and Flame*, Vol. 86, 1991, 383-393.
- <sup>9</sup>Pellett, G. L., Isaac, K. M., Humphreys, W. M., Gartrell, L. R., Roberts, W. L., Dancy, C. L. and Northam, G. B., "Velocity and Thermal Structure, and Strain-Induced Extinction of 14 to 100% Hydrogen-Air Counterflow Diffusion Flames," *Combustion and Flame*, Vol. 112, 1998, 575-592.
- <sup>10</sup>Dixon-Lewis, G., David, T., Gaskell, P. H., Fukutani, S., Jinno, H., Miller, J. A., Kee, R. J., Smooke, M. D., Peters, N., Effelsberg, E., Warnatz, J. and Behrendt, F., "Calculation of the Structure and Extinction Limit of a Methane-air Counterflow Diffusion Flame in the Forward Stagnation Region of a Porous Cylinder," *Proceedings of the Combustion Institute*, Vol. 20, 1984, 1893-1904.
- <sup>11</sup>Tsuji, H. and Yamaoka, I., "The Structure of Counterflow Diffusion Flames in the Forward Stagnation Region of a Porous Cylinder," *Proceedings of the Combustion Institute*, Vol. 12, 1969, 997-1005.
- <sup>12</sup>Seshadri, K., Trevino, C. and Smooke, M. D., "Analysis of the Structure and Mechanisms of Extinction of a Counterflow Methanol-Air Diffusion Flame," *Combustion and Flame*, Vol. 76, 1989, 111-132.
- <sup>13</sup>Chelliah, H. K., Law, C. K., Ueda, T., Smooke, M. D. and Williams, F. A., "An Experimental and Theoretical Investigation of the Dilution, Pressure and Flow-Field Effects on the Extinction Condition of Methane-Air-Nitrogen Diffusion Flames," *Proceedings of the Combustion Institute*, Vol. 23, 1990, 503-511.
- <sup>14</sup>Darabiha, N. and Candel, S., "The Influence of the Temperature on Extinction and Ignition Limits of Strained Hydrogen-Air Diffusion Flames," *Combustion Science and Technology*, Vol. 86, 1992, 67-85.

- <sup>15</sup>Ishizuka, S., "An Experimental study on the opening of Laminar Diffusion Flame Tips," *Proceedings of the Combustion Institute*, Vol. 19, 1982, 319-326.
- <sup>16</sup>Ishizuka, S. and Sakai, Y., "Structure and Tip-Opening of Laminar Diffusion Flames," *Proceedings of the Combustion Institute*, Vol. 21, 1986, 1821-1828.
- <sup>17</sup>Takagi, T. and Xu, Z., "Numerical Analysis of Laminar Diffusion Flames - Effects of Preferential Diffusion of Heat and Species," *Combustion and Flame*, Vol. 96, 1996, 50-59.
- <sup>18</sup>Takagi, T., Xu, Z. and Komiyama, M., "Preferential Diffusion Effects on the Temperature in Usual and Inverse Diffusion Flames," *Combustion and Flame*, Vol. 106, 1996, 252-260.
- <sup>19</sup>Im, H. G., Law, C. K. and Axelbaum, R. L., "Opening of the Burke-Schumann Flame Tip and the effects of Curvature on Diffusion Flame Extinction," *Proceedings of the Combustion Institute*, Vol. 23, 1990, 551-558.
- <sup>20</sup>Rolon, J. C., Aguerre, F. and Candel, S., "Experiments on the Interaction between a Vortex and a Strained Diffusion Flame," *Combustion and Flame*, Vol. 100, 1995, 422-429.
- <sup>21</sup>Takagi, T., Yoshikawa, Y., Yoshida, K., Komiyama, M. and Kinoshita, S., "Studies on Strained Non-Premixed Flames Affected by Flame Curvature and Preferential Diffusion," *Proceedings of the Combustion Institute*, Vol. 26, 1996, 1103-1110.
- <sup>22</sup>Yoshida, K. and Takagi, T., "Transient Local Extinction and Reignition Behavior of Diffusion Flames Affected by Flame Curvature and Preferential Diffusion," *Proceedings of the Combustion Institute*, Vol. 27, 1998, 685-692.
- <sup>23</sup>Finke, H. and Grünefeld, G., "An Experimental Investigation of Extinction of Curved Laminar Hydrogen Diffusion Flames," *Proceedings of the Combustion Institute*, Vol. 28, 2000, 2133-2140.
- <sup>24</sup>Hu, S., Wang, P., Pitz, R. W. and Smooke, M. D., "Experimental and Numerical Investigation of Non-Premixed Tubular Flames," *Proceedings of the Combustion Institute*, Vol. 31, in press, 2006.
- <sup>25</sup>Dongworth, M. and Melvin, A., "Transition to Instability in a Steady Hydrogen-Oxygen Diffusion Flame," *Combustion Science and Technology*, Vol. 14, 1976, 177-182.
- <sup>26</sup>Chen, R.-h., Mitchell, G. B. and Ronney, P. D., "Diffusive-Thermal Instability and Flame Extinction in Nonpremixed Combustion," *Proceedings of the Combustion Institute*, Vol. 24, 1992, 213-221.
- <sup>27</sup>Kaiser, C., Liu, J.-B. and Ronney, P. D., "Diffusive-Thermal Instability of Counterflow Flames at Low Lewis Number," *38th Aerospace Sciences Meeting and Exhibit*, Reno, NV, 2000, AIAA-2000-0576.
- <sup>28</sup>Jacono, D. L., Papas, P. and Monkewitz, P. A., "Cell Formation in Non-Premixed, Axisymmetric Jet Flames Near Extinction," *Combustion Theory and Modelling*, Vol. 7, No. 4, 2003, 635-644.
- <sup>29</sup>Kim, J. S., Williams, F. A. and Ronney, P. D., "Diffusional-Thermal Instability of Diffusion Flames," *Journal of Fluid Mechanics*, Vol. 327, 1996, 273-301.
- <sup>30</sup>Papas, P., Rais, R. M., Monkewitz, P. A. and Tomboulides, A. G., "Instabilities of Diffusion Flames near Extinction," *Combustion Theory and Modelling*, Vol. 7, No. 4, 2003, 603-633.
- <sup>31</sup>Cheatham, S. and Matalon, M., "A General Asymptotic Theory of Diffusion Flames with Application to Cellular Instability," *Journal of Fluid Mechanics*, Vol. 414, 2000, 105-144.
- <sup>32</sup>Metzener, P. and Matalon, M., "Diffusive-Thermal Instabilities of Diffusion Flames: Onset of Cells and Oscillations," *Combustion Theory and Modelling*, Vol. 10, No. 4, 2006, 701-725.
- <sup>33</sup>Mosbacher, D. M., Wehrmeyer, J. A., Pitz, R. W., Sung, C.-J. and Byrd, J. L., "Experimental and Numerical Investigation of Tubular Flames," *Proceedings of the Combustion Institute*, Vol. 29, 2002, 1479-1486.
- <sup>34</sup>Wang, P., Wehrmeyer, J. A. and Pitz, R. W., "Stretch Rate of Tubular Premixed Flames," *Combustion and Flame*, Vol. 145, 2006, 401-414.
- <sup>35</sup>Liñán, A., "The Asymptotic Structure of Counterflow Diffusion Flames for Large Activation Energies," *Acta Astronautica*, Vol. 1, 1974, 1007-1039.